数理解析研究所講究録 1413 巻 2005 年 201-210

Synchronization of the motion of kinks in two-lane totally asymmetric simple exclusion process with open boundary condition

Tetsuya Mitsudo† and Hisao Hayakawa‡

Department of Physics, Yoshida-south campus, Kyoto University, Sakyo-ku, Kyoto, Japan, 606-8501

Abstract. We study the motion of kinks in a two-lane model of the totally asymmetric simple exclusion process with open boundaries. Once a lane change is allowed, the positions of the kinks become synchronized and diffuse together. We analytically study the motion of the kinks by a decoupled approximation. When we choose the lane change rate asymmetric, the difference of the positions of the kinks become zero, though the difference of the number of particles between lanes remain non-zero.

1. Introduction

We often encounter congestions of pedestrian flows and traffic flows in our daily life. We also observe the stuck of grains in granular flows. It is important to study the mechanism of congestions not only from the industrial point of view but also from the physical point of view. For the sake of scientific research, we need to analyze a simple model which captures the essence of the phenomena.

The asymmetric simple exclusion process (ASEP) is one of the simple models adequate to describe such the transport phenomena [1]. It is a stochastic system of particles moving asymmetrically on a lattice. The simplest limit of ASEP is that the particle is only allowed to hop in one direction, which is called the totally asymmetric simple exclusion process (TASEP).

It is known that the stationary state of one-lane ASEP under open boundary conditions has been obtained exactly [2, 3, 4, 5]. Dynamical properties of TASEP are also studied expensively. The exact solutions of the master equation by Bethe ansatz on an infinite system [6] and a periodic system [7] have been obtained. Furthermore, the current fluctuations in an infinite system and a semi-infinite system [8] are also studied. In the open boundary system, we can draw a phase diagram by the parameters of inflow rate and outflow rate at the boundaries. On the phase boundary between the low density phase and the high density phase, there exists a diffusive domain wall

† mitsudo@scphys.kyoto-u.ac.jp
‡ hisao@yuragi.jinkan.kyoto-u.ac.jp

(kink) [9, 10, 11, 12, 13]. Recently, Takesue *et al* [13] have derived a $f^{-3/2}$ law in the power spectrum based on the random walk picture of the kink, and confirmed its quantative validity from the comparison of the Monte Carlo simulation with their theoritical prediction.

However we little know the properties of a multi-lane ASEP which is more realistic than the one-lane model. There are several two-lane models of TASEP [14, 15]. As used in [14] or [15], a realistic lane changeing rule should refer to the states of the front sites. However, the rule makes us difficult to analyze because we need to construct a transfer matrix to refer to the states of three or four sites, which are the current site, the front site and the side site, or the front site of the other lane added to those three sites. Nobody succeeded in analyzing such the model exactly under open boundary conditions, though Belitsky *et al* [14] successfully analyzed the long-time properties of such the two-lane model in an infinite system. Here, thus, we adopt a simpler model of lane change in which the particle may change lanes when the side site is vacant and do not refer to the front site.

The purpose of this paper is to clarlify the motion of kinks in a two-lane TASEP. To fulfill the analysis, we introduce our model and explain how to specify the position of the kink in the next section. In section 3, we discuss the motion of two kinks based on a decoupling (mean field) approximation. We find that the motion of the kinks are synchronized though the number of particles in one lane is different from that in another lane. We compare the solution with the results of Monte Carlo simulation. In section 4, we discuss the validity of the mean field approximation. We find that the two-point correlation function is small during the relaxation process from the independent motion of two kinks to a synchronized motion of them. In section 5, we conclude our results.

2. Our model

2.1. Introduction of our two-lane model

Our two-lane model is defined on a two lane lattice of $L \times 2$ sites, where L is the length of one lane. We introduce the occupation variable $\tau_{j;\ell}$ where $\tau_{j;\ell} = 1$ and $\tau_{j;\ell} = 0$ represent the occupied state and the vacant state on the jth site in the ℓth lane respectively. The particle move forward by the rate 1 during the time interval $\mathrm{d}t$, if the front site is vacant. We assume that all the particles drift from the left to the right. The open boundary condition is characterized by the inflow rate α_ℓ and the outflow rate β_ℓ. The particle is injected to the system by the rate α_ℓ when the 1st site in the ℓth lane is empty, while the particle extracted from the system by the rate β_ℓ when the Lth site in the ℓth lane is empty. On all sites, the particle is allowed to change lanes only to the neighbouring site. A particle on the 1st(2nd) lane can change lanes by the rate $r_\downarrow(r_\uparrow)$ when the side site in another lane is empty.

We denote the probability of finding the system in configuration $\boldsymbol{\tau} = \{\tau_{1;1}, \tau_{2;1}, \cdots, \tau_{L;2}\}$ by $P(\tau_{1;1}, \tau_{2;1}, \cdots, \tau_{L;2})$. We write the time evolution of the two-lane

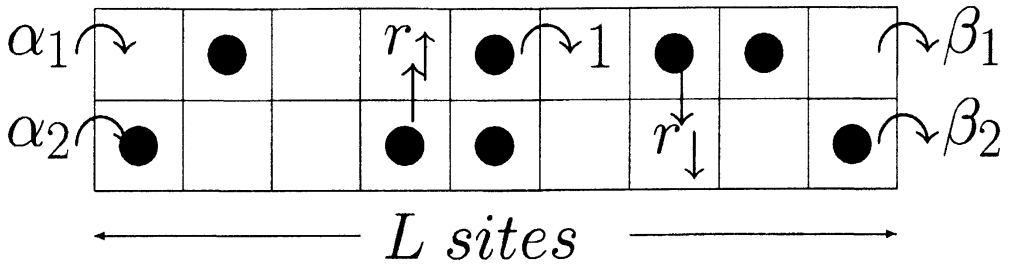

Figure 1. A sample picture of the two-lane model.

model by the master equation,

$$\begin{aligned}\frac{\mathrm{d}}{\mathrm{d}t}P(\tau_{1;1},\cdots,\tau_{L;2}) &= \sum_{\sigma_{1;1}}(h_{1;1})_{\tau_{1;1};\sigma_{1;1}}P(\sigma_{1;1},\cdots,\tau_{L;2}) + \sum_{\sigma_{1;2}}(h_{1;2})_{\tau_{1;2};\sigma_{1;2}}P(\tau_{1;1},\cdots,\tau_{1;2},\cdots,\tau_{L;2}) \\ &+ \sum_{\ell=1}^{2}\sum_{j=1}^{L-1}\sum_{\sigma_{j;\ell},\sigma_{j+1;\ell}}(h_{j,j+1;\ell})_{\tau_{j;\ell},\tau_{j+1;\ell};\sigma_{j;\ell},\sigma_{j+1;\ell}}P(\tau_{1;1},\cdots,\sigma_{j;\ell},\sigma_{j+1;\ell},\cdots,\tau_{L;2}) \\ &+ \sum_{\sigma_{L;1}}(h_{L;1})_{\tau_{L;1};\sigma_{L;1}}P(\tau_{1;1},\cdots,\sigma_{L;1},\cdots,\tau_{L;2}) + \sum_{\sigma_{L;2}}(h_{L;2})_{\tau_{L;2};\sigma_{L;2}}P(\tau_{1;2},\cdots,\sigma_{L;2}) \\ &+ \sum_{j=1}^{L}\sum_{\sigma_{j;1},\sigma_{j;2}}(h_{j;1,2})_{\sigma_{j;1},\sigma_{j;2};\tau_{j;1},\tau_{j;2}}P(\tau_{1;1},\cdots,\sigma_{j;1},\cdots,\sigma_{j;2},\cdots,\tau_{L;2}) \end{aligned} \tag{1}$$

where $\sigma_{j;\ell}$ is used for a dummy variable in the summation, and the transition matrices $h_{1;\ell}, h_{L;\ell}, h_{j,j+1;\ell}, h_{j;1,2}$ are represented as

$$h_{1,\ell} = \begin{pmatrix} -\alpha_\ell & 0 \\ \alpha_\ell & 0 \end{pmatrix}_{1;\ell} \qquad h_{L,\ell} = \begin{pmatrix} 0 & \beta_\ell \\ 0 & -\beta_\ell \end{pmatrix}_{L;\ell}$$

$$h_{j,j+1;\ell} = \begin{pmatrix} 0 & 0 & 0 & 0 \\ 0 & 0 & 1 & 0 \\ 0 & 0 & -1 & 0 \\ 0 & 0 & 0 & 0 \end{pmatrix}_{j,j+1;\ell} \qquad h_{j;1,2} = \begin{pmatrix} 0 & 0 & 0 & 0 \\ 0 & -r_\uparrow & r_\downarrow & 0 \\ 0 & r_\uparrow & -r_\downarrow & 0 \\ 0 & 0 & 0 & 0 \end{pmatrix}_{j;1,2} . \tag{2}$$

Here the density profile $\langle\tau_{j;\ell}\rangle$ and two-point function $\langle\tau_{j;\ell}\tau_{k;\ell'}\rangle$ are defined by,

$$\langle\tau_{j;\ell}\rangle = \sum_{\boldsymbol{\tau}}\tau_{j;\ell}P(\tau_{1;1},\cdots,\tau_{L;2}) \tag{3}$$

$$\langle\tau_{j;\ell}\tau_{k;\ell'}\rangle = \sum_{\boldsymbol{\tau}}\tau_{j;\ell}\tau_{k;\ell'}P(\tau_{1;1},\cdots,\tau_{L;2}), \tag{4}$$

where the summation is taken over all the configurations. The time evolution of $\langle\tau_{j;\ell}\rangle$ is written as

$$\frac{\mathrm{d}}{\mathrm{d}t}\langle\tau_{j;\ell}\rangle = J_{j-1,j;\ell} - J_{j,j+1;\ell} - J_{j;\ell\to\ell'} + J_{j;\ell'\to\ell} \tag{5}$$

for $\ell' \neq \ell$, where the current $J_{j,j+1;\ell}$ between site j and $j+1$ is

$$J_{j,j+1;\ell} = \langle\tau_{j;\ell}(1-\tau_{j+1;\ell})\rangle \tag{6}$$

and the currents between lanes are

$$J_{j;1\to 2} = r_\downarrow \langle \tau_{j;1}(1-\tau_{j;2})\rangle \qquad J_{j;2\to 1} = r_\uparrow \langle \tau_{j;2}(1-\tau_{j;1})\rangle. \tag{7}$$

2.2. The Position of the Kink

It is known that a kink appears when the inflow rate is equal to the outflow rate and both rates are smaller than $1/2$ in one lane ASEP. The kinks also appear in the two-lane model when $\alpha_1 = \beta_1 < 1/2$ and $\alpha_2 = \beta_2 < 1/2$. For $r_\uparrow \neq 0, r_\downarrow \neq 0$, it is obvious that the motion of one kink depend on another kink.

We need to specify the position of the kinks in order to discuss their correlated motion. The position of a stable kink in one-lane ASEP can be determined by using the second class particle [9, 10]. However, we adopt another method to determine the position of the kink by the whole number of particles in a lane. This definition has been used in the domain wall theory [11, 12, 13], and give the exact position of the kink when the inflow and outflow rates are small. The advantage to adopt this method is that it is much simpler and concise than using the second class particle.

We introduce $\langle N_\ell \rangle$ for the whole number of particles in each lane

$$\langle N_\ell \rangle = \sum_{j=1}^{L} \langle \tau_{j;\ell} \rangle. \tag{8}$$

We also introduce $\langle N_G \rangle$ and $\langle N_R \rangle$ by $\langle N_G \rangle = \langle N_2 \rangle + \langle N_1 \rangle$ and $\langle N_R \rangle = \langle N_2 \rangle - \langle N_1 \rangle$ respectively. The position of the kink x_ℓ is defined from the equation based on a kink picture;

$$x_\ell = \frac{\langle N_\ell \rangle - \rho_{\ell;+} L}{\rho_{\ell;-} - \rho_{\ell;+}}, \tag{9}$$

where $\rho_{\ell;\pm}$ represent the density of the ℓth lane. The index $+$ represents the right side of the position of the kink and index $-$ represents the left side of the position of the kink. It is straightforward to give the equation (9) by summing up the equation

$$\langle \tau_{j;\ell} \rangle = \rho_{\ell;-} + (\rho_{\ell;+} - \rho_{\ell;-})\theta(j - x_\ell) \tag{10}$$

from $j = 1$ to L, where $\theta(z)$ is the step function,

$$\theta(z) = \begin{cases} 1 & \text{for } z \geq 0 \\ 0 & \text{for } z < 0 \end{cases}. \tag{11}$$

Thus, once $\langle N_\ell \rangle$ is known, we can determine the position of the kink.

3. Mean-Field Theory

For the large system size L, we can neglect the boundary terms. Thus the equations for $\langle N_G \rangle, \langle N_R \rangle$ are given by

$$\frac{\mathrm{d}}{\mathrm{d}t}\langle N_G \rangle = 0 \tag{12}$$

$$\frac{\mathrm{d}}{\mathrm{d}t}\langle N_R \rangle = -2r_\uparrow \langle N_R \rangle + 2(r_\downarrow - r_\uparrow) \sum_{j=1}^{L} \langle \tau_{j;1}(1-\tau_{j;2})\rangle. \tag{13}$$

When $r_\downarrow = r_\uparrow$, the equation (13) is reduced to

$$\frac{\mathrm{d}}{\mathrm{d}t}\langle N_R\rangle = -2r_\uparrow\langle N_R\rangle. \tag{14}$$

Thus $\langle N_R\rangle$ relaxes to 0 by an exponential in time, and the number of particles becomes identical in both lanes in the long time limit.

However for $r_\downarrow \neq r_\uparrow$, the problem becomes nontrivial because of the two-point function in the second term in the right hand side of the eq. (13). In general, the two point correlation function is determined by an equation including three point correlation function. Thus, we cannot obtain the exact form of the many-point correlation functions without truncation of the hieralchy of correlation functions. Here we adopt the simplest truncation, which is the decoupling (mean-field) approximation as

$$\sum_{j=1}^{L}\langle\tau_{j;1}(1-\tau_{j;2})\rangle \simeq \sum_{j=1}^{L}\langle\tau_{j;1}\rangle(1-\langle\tau_{j;2}\rangle). \tag{15}$$

We also use the kink picture (10) to approximate the density profile $\langle\tau_{j;\ell}\rangle$.

Let us discuss the motion of two kinks starting from the initial condition where two separated kinks exist in both lanes. The density profile changes in time during the synchronization of the kinks. Furthermore, we assume that the density changes by keeping the density profile (10). Thus we have to determine the time evolution of the density $\rho_{\ell;\pm}$ on the both sides of the kink. By introducing $\rho_{G;\pm} = \rho_{2;\pm} + \rho_{1;\pm}$ and $\rho_{R;\pm} = \rho_{2;\pm} - \rho_{1;\pm}$, the time evolution equations for $\rho_{G;\pm}$ and $\rho_{R;\pm}$ are respectively written as

$$\frac{\mathrm{d}}{\mathrm{d}t}\rho_{G;\pm} = 0 \tag{16}$$

$$\frac{\mathrm{d}}{\mathrm{d}t}\rho_{R;\pm} = -(r_\uparrow + r_\downarrow)\rho_{R;\pm} - \frac{1}{2}(r_\uparrow - r_\downarrow)\rho_{R;\pm}^2 + (r_\downarrow - r_\uparrow)(\rho_{G;\pm} - \frac{\rho_{G;\pm}^2}{2}). \tag{17}$$

Equations (16) and (17) can be solved exactly,

$$\rho_{G;\pm} = \rho_{G;\pm}^0 \tag{18}$$

$$\rho_{R;\pm} = \omega_- + \frac{2\gamma}{\epsilon}\frac{e^{-\gamma t}}{e^{-\gamma t} - C_\pm}, \tag{19}$$

where

$$\epsilon = r_\downarrow - r_\uparrow \qquad \gamma = \frac{1}{2}(r_\downarrow - r_\uparrow)(\omega_+ - \omega_-) \tag{20}$$

$$\omega_\pm = \frac{r_\downarrow + r_\uparrow \pm \sqrt{(r_\downarrow + r_\uparrow)^2 - 2(r_\downarrow - r_\uparrow)^2(\alpha_1 + \alpha_2 - (\alpha_1 + \alpha_2)^2/2)}}{r_\downarrow - r_\uparrow} \tag{21}$$

$$C_\pm = \frac{\rho_{R;\pm}^0 - \omega_+}{\rho_{R;\pm}^0 - \omega_-}. \tag{22}$$

The initial conditions $\rho_{G;\pm}^0$ and $\rho_{R;\pm}^0$ are taken as the stationary densities in one-lane model as

$$\rho_{G;-}^0 = \alpha_1 + \alpha_2 \qquad \rho_{R;-}^0 = \alpha_2 - \alpha_1 \tag{23}$$

$$\rho_{G;+}^0 = 2 - \alpha_1 - \alpha_2 \qquad \rho_{R;+}^0 = \alpha_1 - \alpha_2. \tag{24}$$

Thus we obtain the density $\rho_{\ell;-}$

$$\rho_{1;-} = \rho_1' - \frac{\gamma}{\epsilon}\frac{e^{-\gamma t}}{e^{-\gamma t} - C_-} \qquad \rho_{2;-} = \rho_2' + \frac{\gamma}{\epsilon}\frac{e^{-\gamma t}}{e^{-\gamma t} - C_-} \tag{25}$$

and the density $\rho_{\ell;+}$

$$\rho_{1;+} = 1 - \rho_2' - \frac{\gamma}{\epsilon}\frac{e^{-\gamma t}}{e^{-\gamma t} - C_+} \qquad \rho_{2;+} = 1 - \rho_1' + \frac{\gamma}{\epsilon}\frac{e^{-\gamma t}}{e^{-\gamma t} - C_+} \tag{26}$$

where

$$\rho_1' = \frac{\alpha_1 + \alpha_2 - \omega_-}{2} \qquad \rho_2' = \frac{\alpha_1 + \alpha_2 + \omega_-}{2} \tag{27}$$

Therefore we obtain the time evolution of the density profile $\langle \tau_{j;\ell} \rangle$ for $r_\downarrow \neq r_\uparrow$.

Substituting eq. (10) into (13) with the aid of (15) we obtain,

$$\frac{\mathrm{d}}{\mathrm{d}t}\langle N_R \rangle = -(2r_\uparrow + \epsilon(1 - \rho_{2;-} + \rho_{1;+}))\langle N_R \rangle + 2\epsilon\rho_{1;+}\rho_{2;-}L + \epsilon(1 - \rho_{1;+} - \rho_{2;-})\langle N_G \rangle \tag{28}$$

for $x_1 < x_2$ and

$$\frac{\mathrm{d}}{\mathrm{d}t}\langle N_R \rangle = -(2r_\uparrow + \epsilon(1 - \rho_{2;+} + \rho_{1;-}))\langle N_R \rangle + 2\epsilon\rho_{1;-}\rho_{2;+}L + \epsilon(1 - \rho_{1;-} - \rho_{2;+})\langle N_G \rangle \tag{29}$$

for $x_1 > x_2$. Equations (28) and (29) can be solved exactly, though the expression is lengthy (see (A.4) and (A.5)). Here, we present the solution for $\langle N_R \rangle$ in the long time limit as,

$$\langle N_R \rangle_\infty = \frac{\epsilon\rho_1'(1 - \rho_1')L}{r_\uparrow + \epsilon\rho_1'} \tag{30}$$

for $x_1 > x_2$, and

$$\langle N_R \rangle_\infty = \frac{\epsilon\rho_2'(1 - \rho_2')L}{r_\downarrow - \epsilon\rho_2'} \tag{31}$$

for $x_1 < x_2$. These results show that there remains the mean difference of the number of particles between lanes. The validity of our analysis based on the decoupling approximation is confirmed by the comparison of our result with the Monte Carlo simulation when $|r_\uparrow - r_\downarrow|$ is not large. Figure 2 shows the quantative accuracy of our analysis in the time evolution of $\langle N_R \rangle$.

Though $\langle N_R \rangle$ remains finite, the positions of the kinks are synchronized. In fact, from eqs. (30) or (31) and (9) we obtain,

$$x_2 - x_1 = 0. \tag{32}$$

Thus the positions of the kinks become identical in the long time limit. This result is reasonable, because we cannot choose a preferable congestion front in traffic jams.

4. Discussion

Now let us discuss the validity of the decoupling approximation. Although it is difficult to evaluate the two-point function exactly, it is possible to evaluate it from the Monte Carlo simulation. The result of our simulation for the two-point function

$$A = \frac{\sum_{j=1}^{L}\langle \tau_{j;1}\tau_{j;2} \rangle - \sum_{j=1}^{L}\langle \tau_{j;1} \rangle\langle \tau_{j;2} \rangle}{\sum_{\ell=1}^{2}\sum_{j=1}^{L}\langle \tau_{j;\ell}^2 \rangle} \tag{33}$$

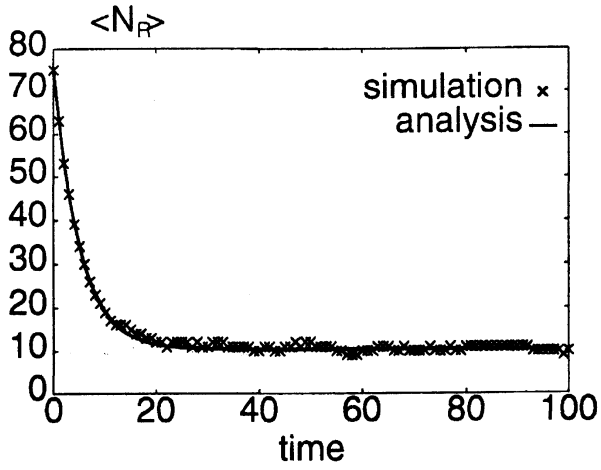

Figure 2. Time evolution comparison between the simulation and the calculation. The solution (A.4) is shown by the solid line and the simulation result is shown by cross. The parameters are $\alpha_1 = \beta_1 = 0.1, \alpha_2 = \beta_2 = 0.15, r_\downarrow = 0.11, r_\uparrow = 0.1, L = 1000$. Time step is taken for each Monte Carlo step. The initial condition is fixed to $\langle N_R \rangle_0 = 75$ and averaged over 1000 samples.

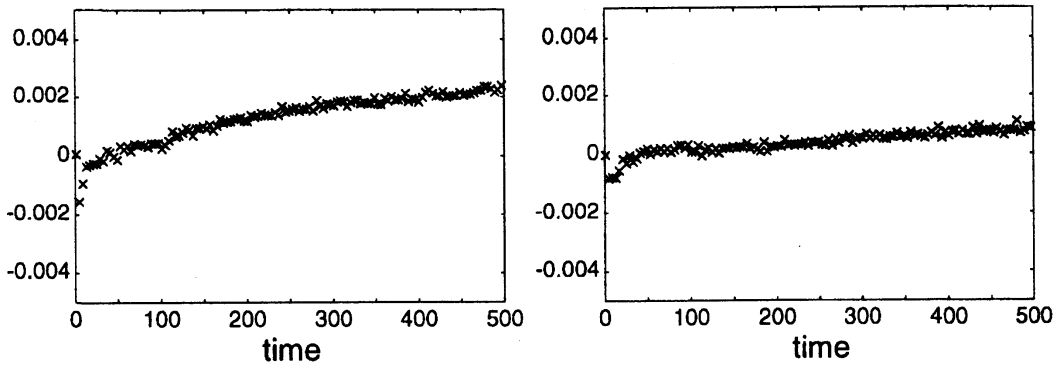

Figure 3. The vertical axis shows the value A obtained from the simulations and the horizontal axis shows the time. The simulation is done when $r_\downarrow = 0.11, r_\uparrow = 0.1$ (figure on the left and the solution match) and $r_\downarrow = 0.03, r_\uparrow = 0.01$ (figure on the right and the solution does not match). In both cases, the boundary parameters are taken as $\alpha_1 = \beta_1 = 0.1, \alpha_2 = \beta_2 = 0.15$, the system size $L = 1000$, and averaged over 1000 samples.

is shown in Fig.3. In the left figure of Fig.3, we realize that A is small between $t = 30$ and $t = 100$. The synchronization is realized before $t = 30$ as we can see in Fig.2. Thus, we may expect that the decoupling approximation adopted here works well to describe the synchronization of the kinks.

However there is a certain parameter region that the decoupling approximaiton fails. In fact, the left figure of Fig.4 shows $\langle N_R \rangle$ obtained from the simulation deviates from that in the decoupling approximation. The positions of the kinks are not identical in this case. The value A given by the simulation in the Fig.3(right) when it deviates

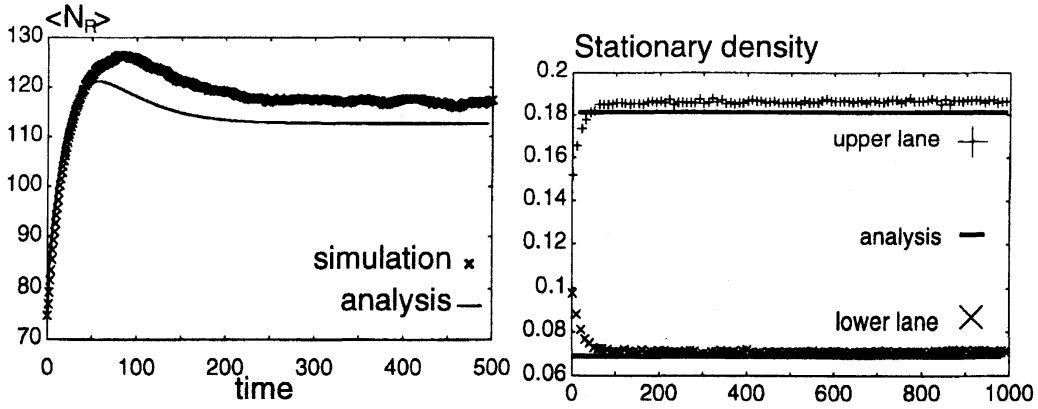

Figure 4. The figure in the left shows the time evolution of $\langle N_- \rangle$ when the analysis fails. The difference from the case in fig.3 is only the lane changing rate; $r_\downarrow = 0.03, r_\uparrow = 0.01$. The figure in the right shows the difference between the stationary density given by the simulation and by the equation (17), in the corresponding low density region. The boundary parameters are $\alpha_1 = 0.1, \beta_1 = 0.9, \alpha_2 = 0.15, \beta_2 = 0.85$.

from the decoupling approximation. The value A is almost 0 in the region between $t = 30$ and $t = 200$. This deviation can be explained by the violation of the decoupled approximation in the density evolution equation (17). There is a region that the stationary density $\rho_{\ell;\pm}$ is not given by the eq. (17). The comparison of $\rho_{\ell;-}$ between the result of the simulation and the solution of the equation (17) is shown in Fig.4(right). We can see that the density derived from the mean-field theory deviates from the result of the simulation. Thus in the region that the final densities of each lane differ from the solutions of the eq. (17), the final positions of the kinks are not identical. To discuss such the region, we need more precise analysis.

5. Conclusion

In this paper, we have studied the motion of kinks in the two-lane TASEP. We obtain the explicit time evolution function of the average number of particles in each lane which is related to the position of the kink by adopting the decoupling approximation of the two-point correration function. We find that the positions of the kinks are synchronized, though the number of particles in a lane can be different from that in another lane. We confirm the validity of our analysis by compairing the result of the Monte Carlo simulation and the analytical result.

We would like to thank S.Takesue for fruitful discussion. This work is partialy supported by the Grant-in-Aid for Scientific Research (Grant No. 15540393) of the Ministry of Education, Culture, Sports, Science and Technology(MEXT), Japan, and the Grant-in-Aid for the 21st century COE 'Center for Diversity and Universality in Physics' from MEXT, Japan.

Appendix A. The calculation of $\langle N_R \rangle$

In this appendix, we give the explicite expression of $\langle N_R \rangle$. Equation (29) is solved as

$$\langle N_R \rangle = \langle N_R \rangle_0 e^{-\int_0^t \mathrm{d}t'(2r_\uparrow + \epsilon(1-\rho_{2;+}+\rho_{1;-}))} + \epsilon \int_0^t \mathrm{d}t' e^{\int_t^{t'} \mathrm{d}t''(2r_\uparrow+\epsilon(1-\rho_{2;+}+\rho_{1;-}))}(2L\rho_{1;-}\rho_{2;+} + (1-\rho_{1;-}-\rho_{2;+})\langle N_G \rangle) \quad \text{(A.1)}$$

Here, we perform the integral in the argument of the exponential function,

$$\int_0^t \mathrm{d}t'(1-\rho_{2;+}+\rho_{1;-}) = 2\rho_1' t + \frac{1}{\epsilon}\ln\left(\frac{(C_+ - e^{-\gamma t})(C_- - e^{-\gamma t})}{C_+ C_-}\right). \quad \text{(A.2)}$$

Therefore,

$$e^{-\int_0^t \mathrm{d}t'(2r_\uparrow+\epsilon(1-\rho_{2;+}+\rho_{1;-}))} = e^{-2(r_\uparrow+\epsilon\rho_1')t}\frac{C_+C_-}{(C_+ - e^{-\gamma t})(C_- - e^{-\gamma t})}. \quad \text{(A.3)}$$

After executing the calculation, we finally achieve

$$\begin{aligned}\langle N_R \rangle = {} & \langle N_R \rangle_0 e^{-2(r_\uparrow+\epsilon\rho_1')t}\frac{C_+C_-}{(C_+ - e^{-\gamma t})(C_- - e^{-\gamma t})} \\ & + \frac{\epsilon}{(C_+ - e^{-\gamma t})(C_- - e^{-\gamma t})}\left[L\rho_1'(1-\rho_1')C_+C_-\frac{1-e^{-2(r_\uparrow+\epsilon\rho_1')}}{r_\uparrow+\epsilon\rho_1'}\right. \\ & + \frac{e^{-\gamma t}-e^{-2(r_\uparrow+\epsilon\rho_1')}}{2(r_\uparrow+\epsilon\rho_1')-\gamma}2L\left(\frac{\gamma}{\epsilon}(C_+ - \rho_1'(C_- + C_+)) - (C_- + C_+)\rho_1'(1-\rho_1')\right) \\ & + \frac{e^{-\gamma t}-e^{-2(r_\uparrow+\epsilon\rho_1')}}{2(r_\uparrow+\epsilon\rho_1')-\gamma}\frac{\gamma}{\epsilon}(C_- - C_+)\langle N_G \rangle \\ & \left. + \frac{e^{-2\gamma t}-e^{-2(r_\uparrow+\epsilon\rho_1')}}{r_\uparrow+\epsilon\rho_1'-\gamma}\left(-\frac{\gamma^2}{\epsilon^2}+\frac{\gamma}{\epsilon}(2\rho_1'-1)+\rho_1'(1-\rho_1')\right)L\right] \end{aligned} \quad \text{(A.4)}$$

for $x_1 > x_2$, and

$$\begin{aligned}\langle N_R \rangle = {} & \langle N_R \rangle_0 e^{-2(r_\downarrow-\epsilon\rho_2')t}\frac{C_+C_-}{(C_+ - e^{-\gamma t})(C_- - e^{-\gamma t})} \\ & + \frac{\epsilon}{(C_+ - e^{-\gamma t})(C_- - e^{-\gamma t})}\left[L\rho_2'(1-\rho_2')C_-C_+\frac{1-e^{-2(r_\downarrow-\epsilon\rho_2')}}{r_\downarrow-\epsilon\rho_2'}\right. \\ & + \frac{e^{-\gamma t}-e^{-2(r_\downarrow-\epsilon\rho_2')}}{2(r_\downarrow-\epsilon\rho_2')-\gamma}2L\left(\frac{\gamma}{\epsilon}(C_+ + \rho_2'(C_- - C_+)) - (C_- + C_+)\rho_2'(1-\rho_2')\right) \\ & + \frac{e^{-\gamma t}-e^{-2(r_\downarrow-\epsilon\rho_2')}}{2(r_\downarrow-\epsilon\rho_2')-\gamma}\frac{\gamma}{\epsilon}(C_- - C_+)\langle N_G \rangle \\ & \left. + \frac{e^{-2\gamma t}-e^{-2(r_\downarrow-\epsilon\rho_2')}}{r_\downarrow-\epsilon\rho_2'-\gamma}\left(-\frac{\gamma^2}{\epsilon^2}+\frac{\gamma}{\epsilon}(2\rho_2'-1)+\rho_2'(1-\rho_2')\right)L\right] \end{aligned} \quad \text{(A.5)}$$

for $x_1 < x_2$.

References

[1] Schütz G M 2001*Exact Solvable Models for Many-Body Systems Far from Equilibrium, in Phase Transitions and Critical Phenomena* Vol.19 ed Domb C and Lebowitz J L,(Academic,London)

[2] Derrida B,Evans M R,Hakeem V and Pasquier V 1993 *J.Phys.A* **26** 1493
[3] Schütz G M and Domany E 1993 *J.Stat.Phys* **72** 277
[4] Sasamoto T 1999 *J.Phys.A* **32** 7109
[5] Uchiyama M, Sasamoto S and Wadati M 2004 *J.Phys.A* **37** 4958
[6] Schütz G M 1997 *J.Stat.Phys* **88** 427
[7] Priezzhev V B 2003 *Phys.Rev.Lett* **91** 050601
[8] Prähofer M and Spohn H 2002 *In and out of equilibrium* **51** ed. V.Sidoravicious 185
[9] Derrida B, Lebowitz J L, and Speer E R 1997 *J.Stat.Phys* **89** 135
[10] Ferrari P A 1992 *Prob.Theo.Rel.Fields* **91** 81
[11] Kolomeisky A B, Schütz G M, Kolomeisky E B and Straley J P 1998 *J.Phys.A* **31** 6911
[12] Santen L and Appert C 2002 *J.Stat.Phys* **106** 187
[13] Takesue S, Mitsudo T, and Hayakawa H 2003 *Phys.Rev.*E **68** 01930R
[14] Belitsky V, Krug J, Neves E J and Schütz G M 2001 *J.Stat.Phys* **103** 945
[15] Nagatani T 1996 *J.Phys.A* **29** 6531